Electronic Supplementary Material (ESI) for CrystEngComm.

Supporting Information

Highly tunable emission properties of solid state supramolecular compounds based on Eu-mixed lanthanide complexes and cucurbit[6]uril

Mariana I. Rakhmanova,[a] Taisiya S. Sukhikh[a], Ekaterina A. Kovalenko[a]*

[a]Nikolaev Institute of Inorganic Chemistry, Siberian Branch of the Russian Academy of Sciences, 3, Academician Lavrentiev Avenue, Novosibirsk 630090, Russian Federation

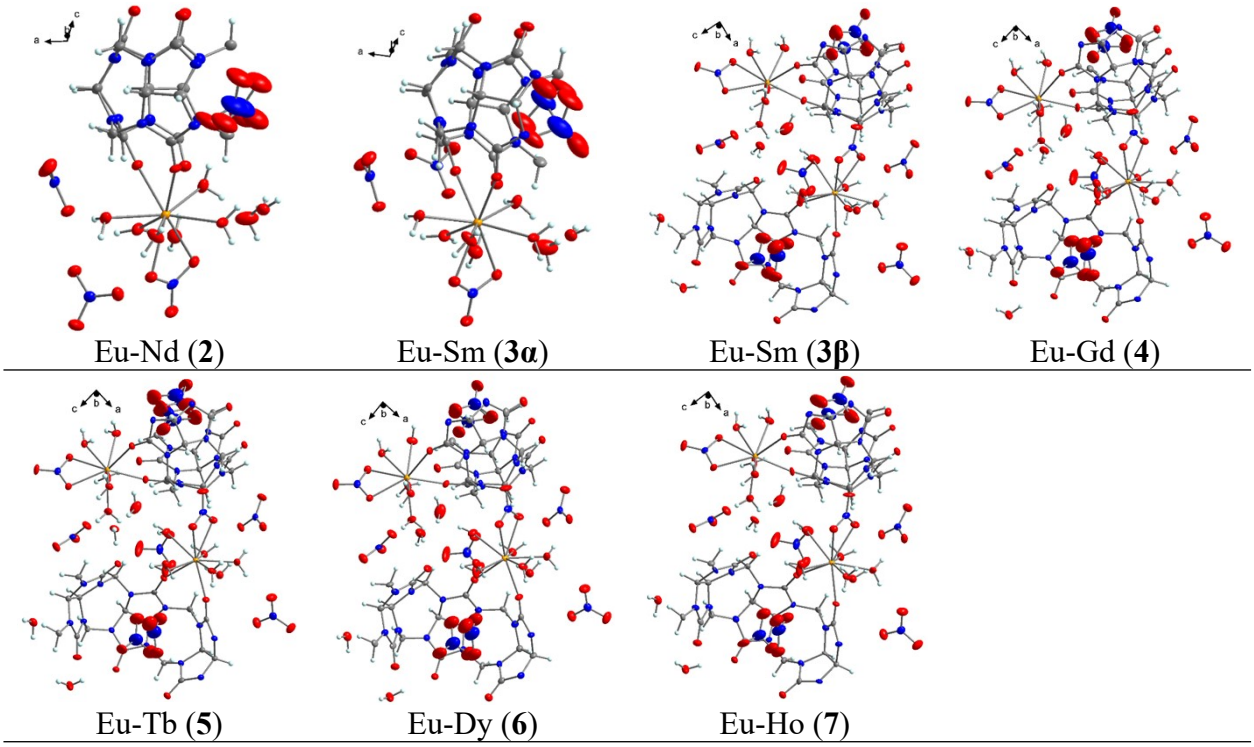

Figure S1. Representation of atomic displacement ellipsoids (50% probability) for non-hydrogen atoms in the crystallographically independent part of the structures. Hydrogen atoms are shown as spheres of fixed size. Each of the disordered nitrates located in the cavity of CB[6] is further disordered over two positions due to the proximity to the special position.

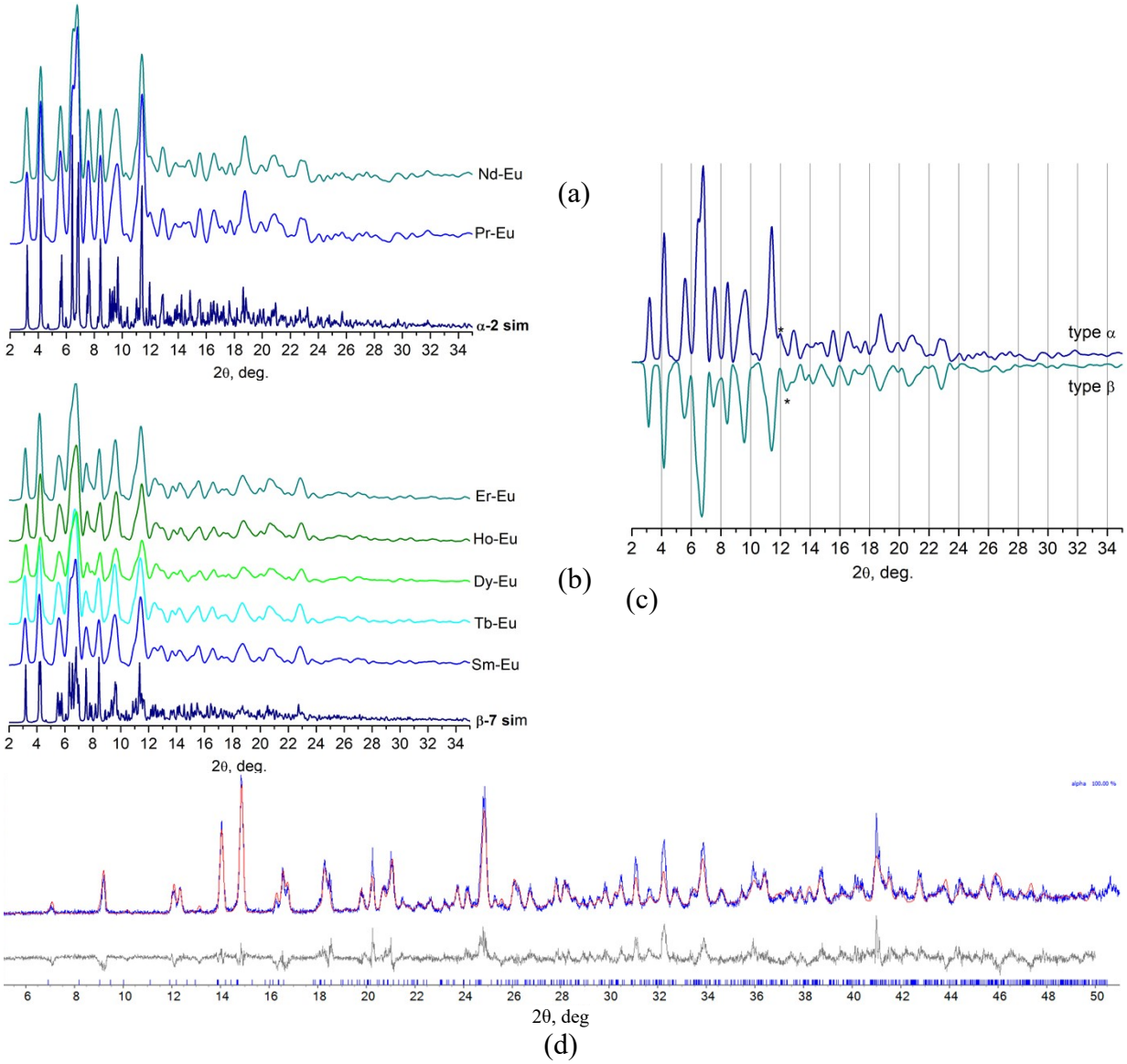

Fig. S2. Simulated and experimental (Mo Kα radiation, 150 K) powder XRD patterns for type α (a) compounds **1**, **2** and β (b) compounds **3**–**8**, and their comparison (c) showing slight differences. (d) Rietveld refinement for a sample [Eu-Pr]: the experimental pattern (Cu Kα radiation, 298 K; blue), simulated pattern (red) and the difference (gray). Refined unit cell parameters: $P2_1/n$, a = 14.5417(4) Å, b = 13.6308(7) Å, c = 18.3293(7) Å, β = 105.476(3)°, V = 3501.4(2) Å^3. Atomic positions were fixed to be the same as in the single-crystal structure. Some differences of the peak intensities can be due to a slight variation of atomic positions; applying spherical harmonic (order 4) preferred orientation functions does not completely eliminate the difference.

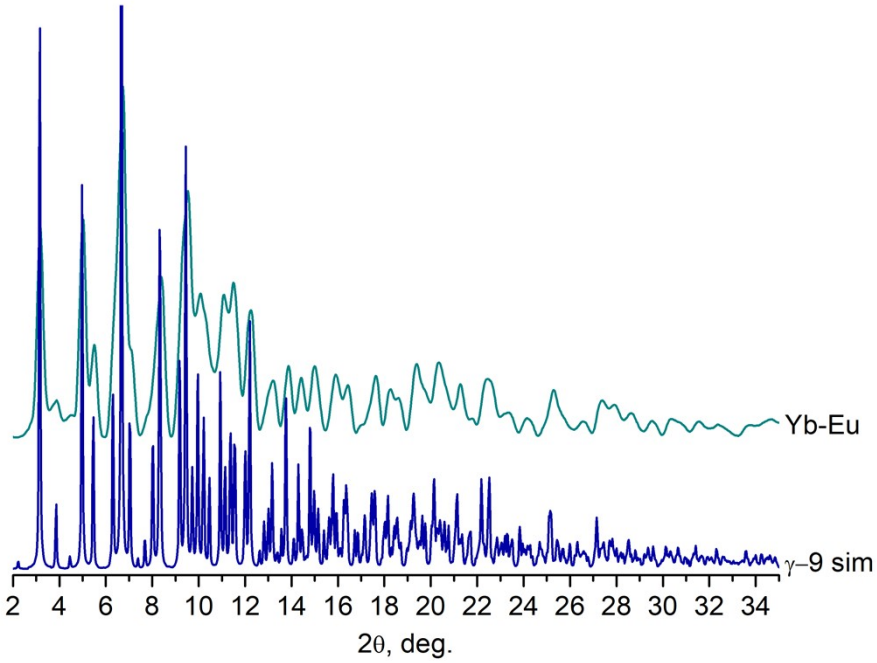

Fig. S3. Simulated and experimental (Mo Kα radiation) powder XRD patterns for type γ compound

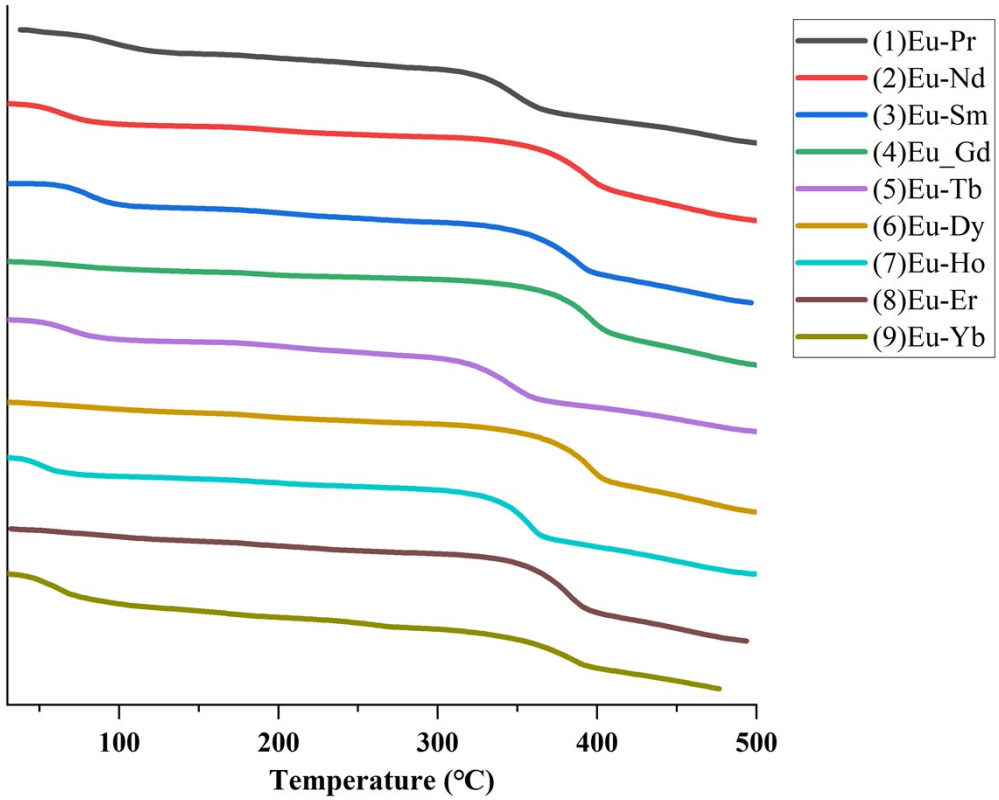

Fig. S4a. The TGA curves of compounds **1**–**9**.

Fig. S4b. The TGA curve of compound Eu-Pr (1)

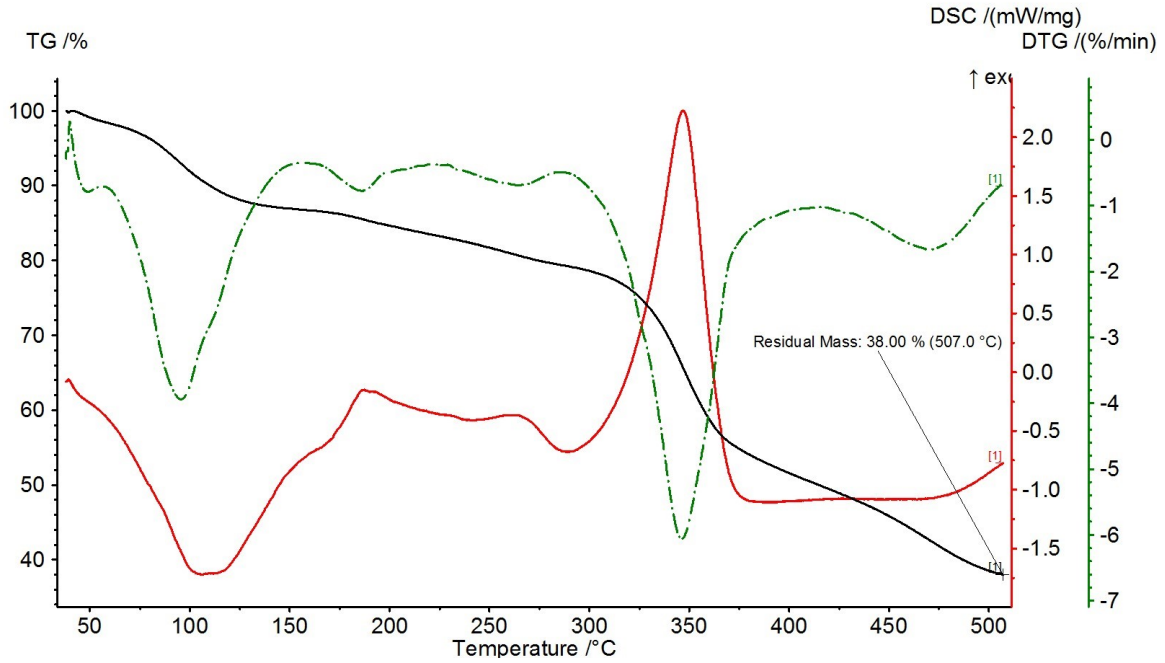

Thermal decomposition of compound **1**. First, dehydration occurs in the temperature range of 55–150°C and is accompanied by a 10 % weight loss of eight crystallization water molecules. In the temperature range of 160–300°C, the sample gradually is decomposed, being accompanied by loss of crystallization nitric acid molecules. Further weight loss occurs at 350°C, which corresponds to the decomposition temperature of CB[6].

Fig. S4c. The TGA curve of compound Eu-Nd (2)

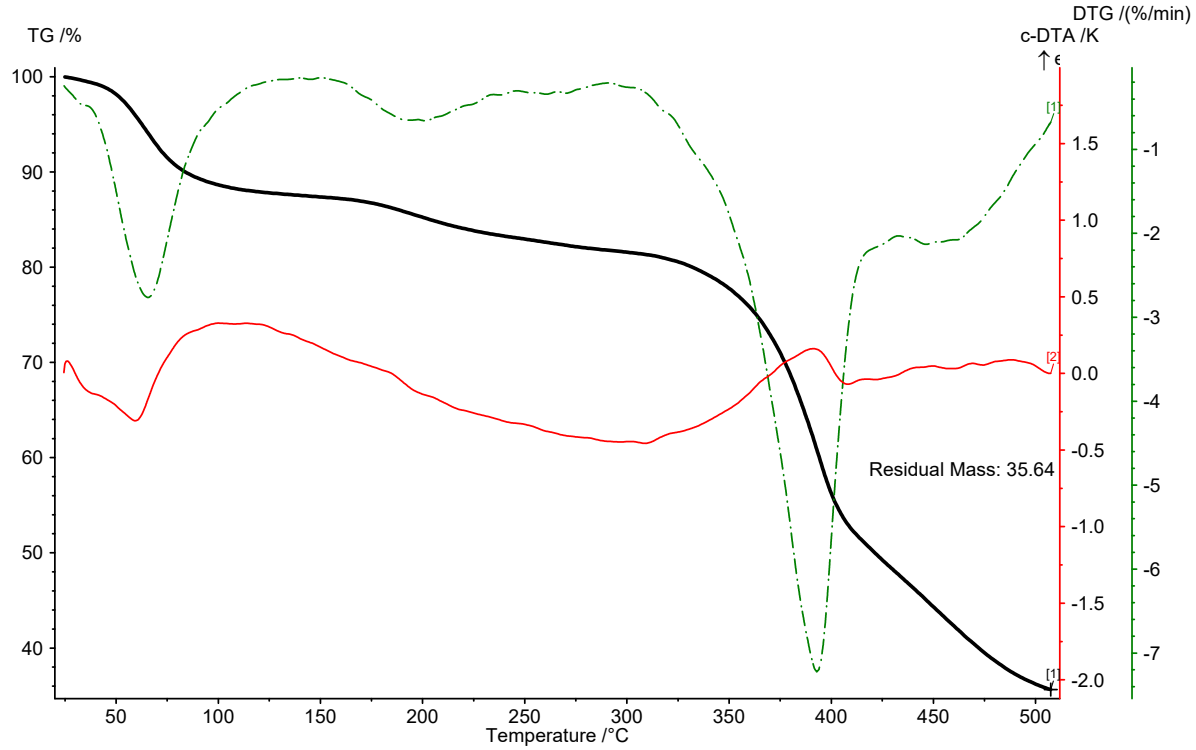

Thermal decomposition of **2** begins at 55–60°C . Desolvation occurs in the temperature range of 60–100°C, being accompanied by a 9 % weight loss of the eight crystallization water. At temperature 150°C compound loose one crystallization nitric acid molecule. In the temperature ranges of 200–350°, the sample is gradually decomposed. Further weight loss occurs at 390°C, which corresponds to the decomposition temperature of CB[6].

Fig. S4d. The TGA curve of compound Eu-Sm (3)

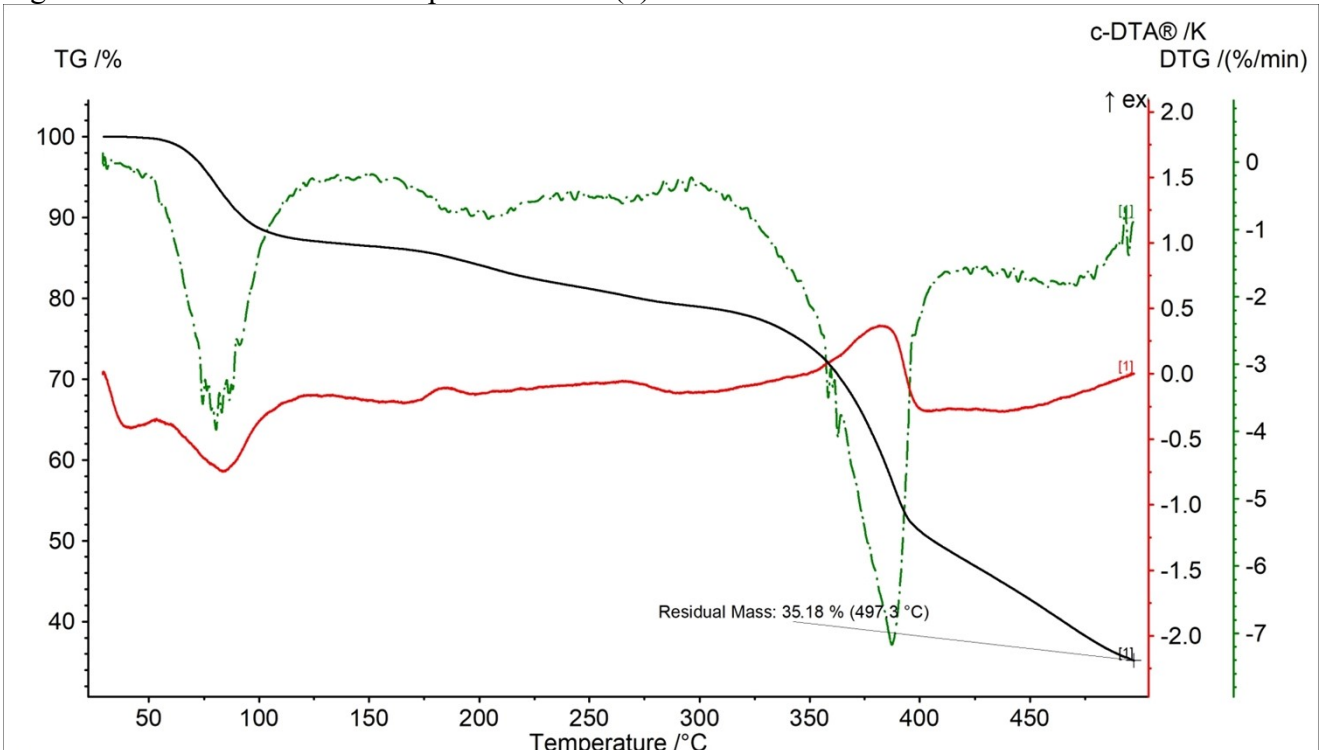

Thermal decomposition of compound **3**. Desolvation occurs in the temperature range of 55–100°C, being accompanied by a 12 % weight loss of the ten crystallization water. At temperature 150°C compound loose one crystallization nitric acid molecule. In the temperature ranges of 200–350°, the sample is gradually decomposed. Further weight loss occurs at 390°C, which corresponds to the decomposition temperature of CB[6].

Fig. S4e. The TGA curve of compound Eu-Gd (4)

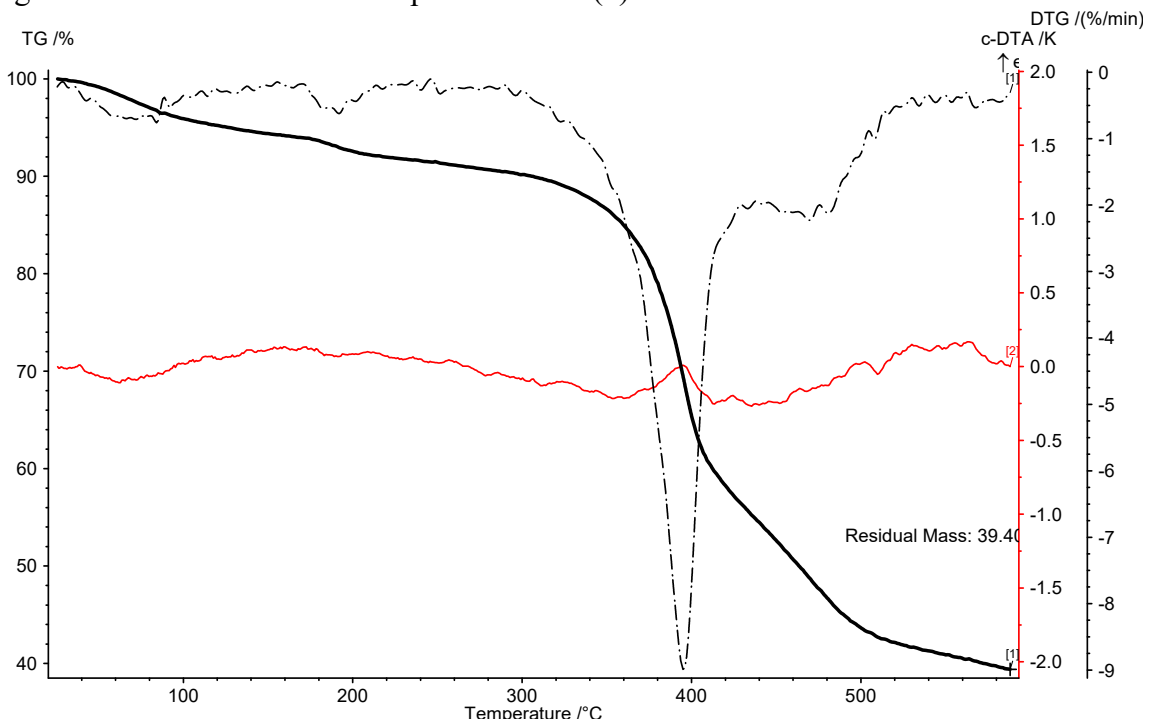

On the mass loss curve of compound **4** we observe the gradual thermal decomposition of the sample in the temperature range of 50–300°C and is accompanied by a 8 % weight loss of six crystallization water molecules and crystallization nitric acid molecules. Further weight loss occurs at 395°C, which corresponds to the decomposition temperature of CB[6].

Fig. S4f. The TGA curve of compound Eu-Tb (5)

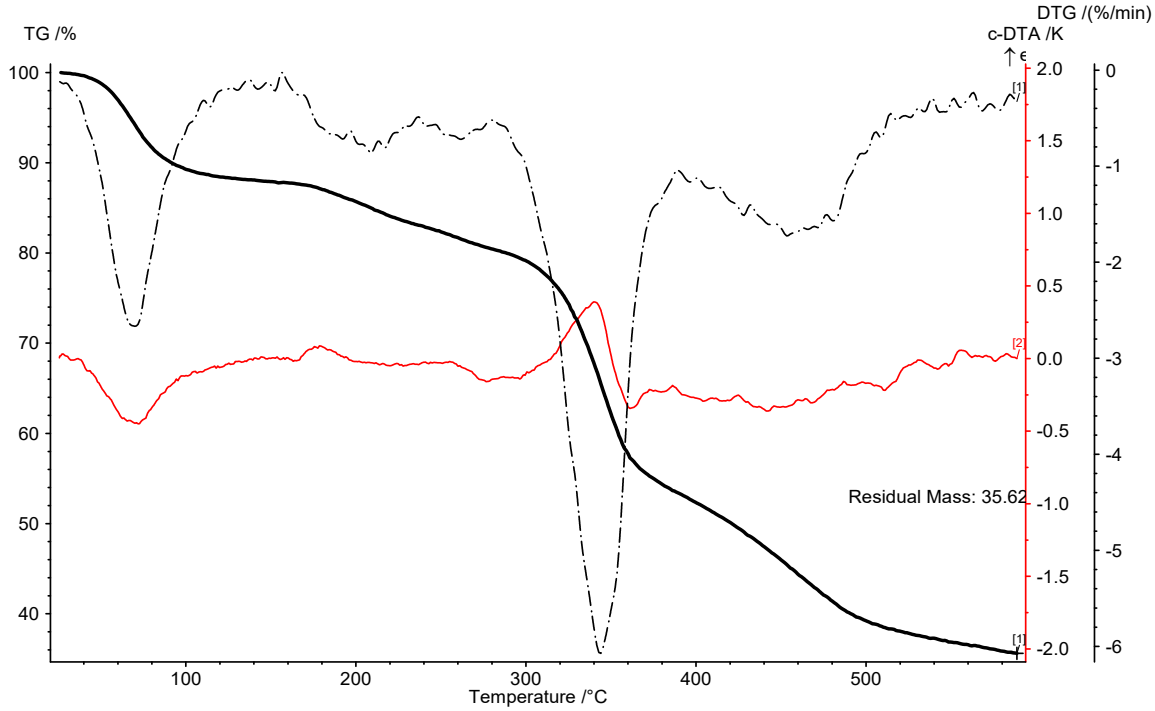

Thermal decomposition of compound **5**. First, dehydration occurs in the temperature range of 45–95°C and is accompanied by a 8 % weight loss of seven crystallization water molecules. In the temperature range of 160–240°C, the sample gradually is decomposed, being accompanied by loss of crystallization nitric acid molecules. Further weight loss occurs at 340°C, which corresponds to the decomposition temperature of CB[6].

Fig. S4g. The TGA curve of compound Eu-Dy (6)

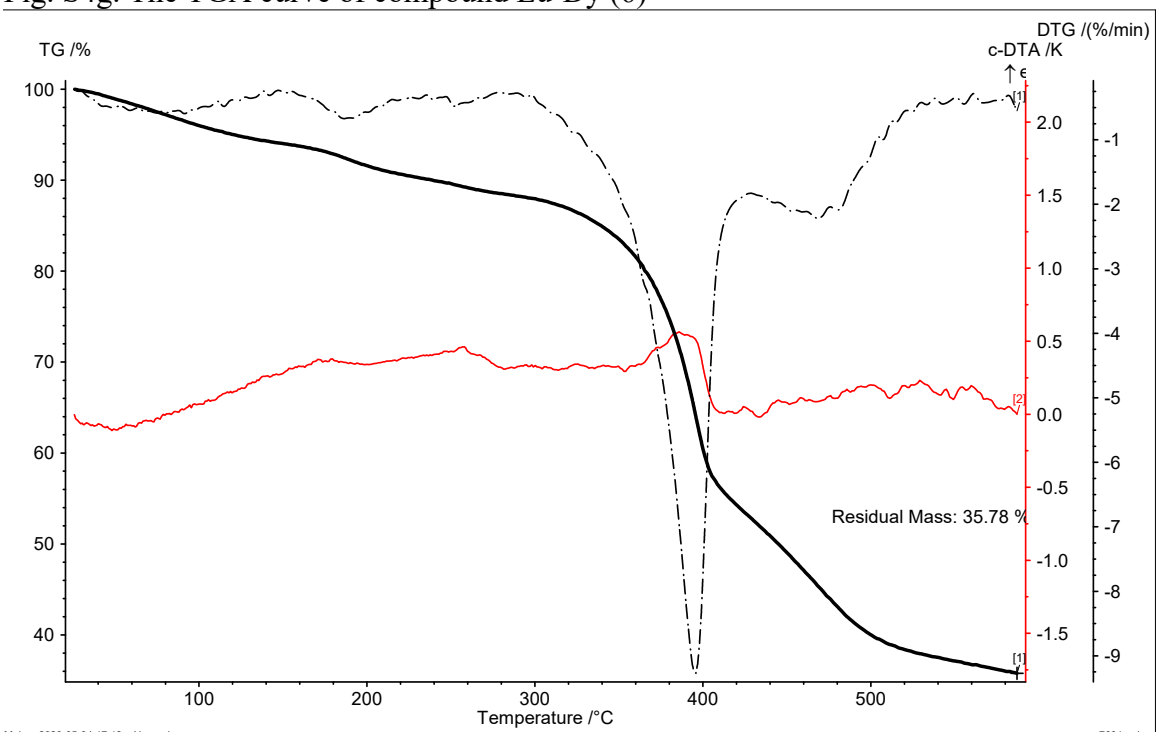

On the mass loss curve of compound **6** we observe the gradual thermal decomposition of the sample in the temperature range of 50–300°C and is accompanied by a 10 % weight loss of six crystallization water molecules and crystallization nitric acid molecules. Further weight loss occurs at 400°C, which corresponds to the decomposition temperature of CB[6].

Fig. S4h. The TGA curve of compound Eu-Ho (7)

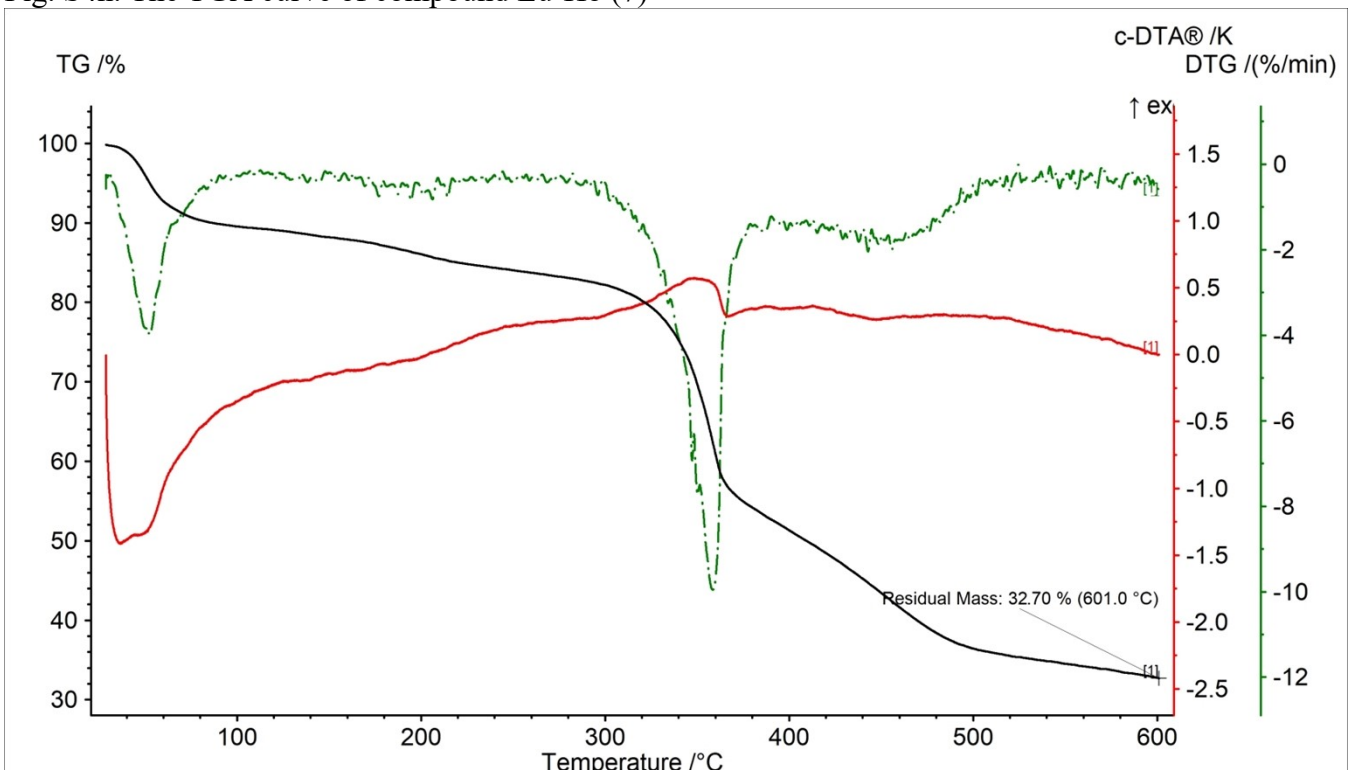

Thermal decomposition of compound **7**. Desolvation occurs in the temperature range of 40–80°C, being accompanied by a 6 % weight loss of the five crystallization water. At temperature 200°C compound loose one crystallization nitric acid molecule. Further weight loss occurs at 360°C, which corresponds to the decomposition temperature of CB[6].

Fig. S4i. The TGA curve of compound Eu-Er (8)

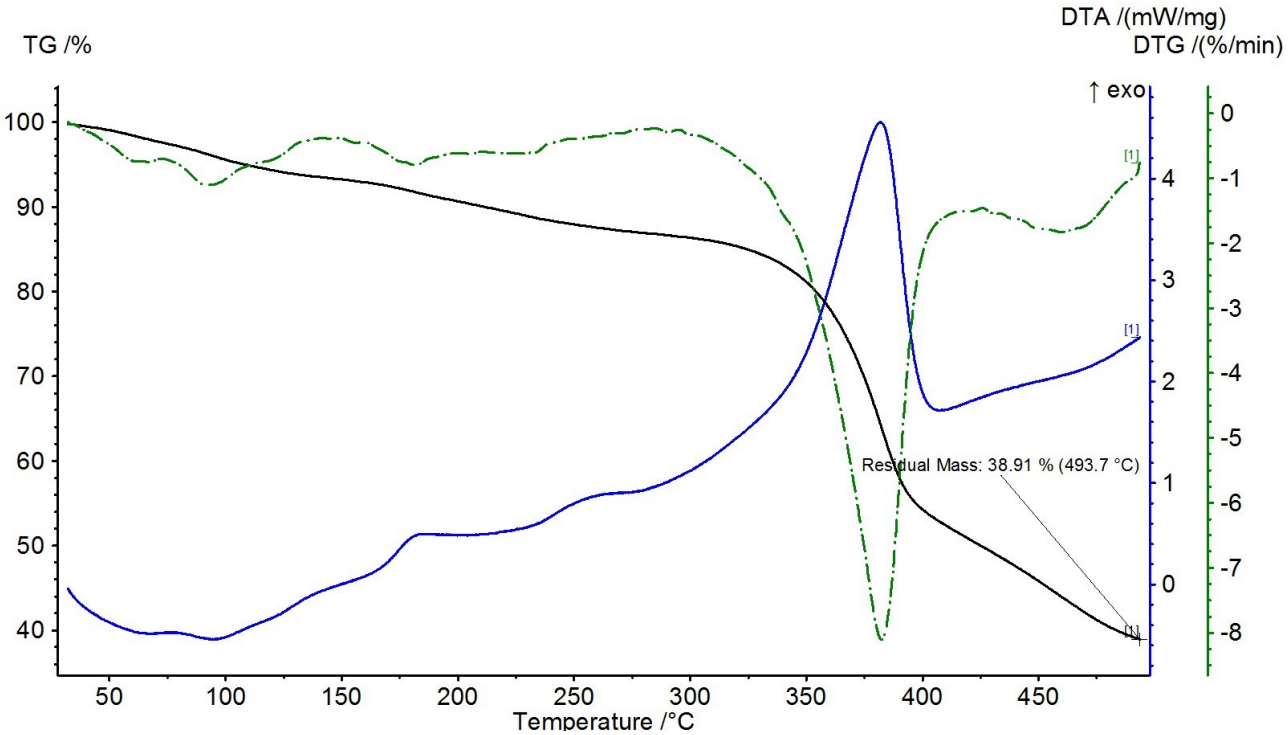

On the mass loss curve of compound **8** we observe the gradual thermal decomposition of the sample in the temperature range of 50–300°C and is accompanied by a 12 % weight loss of ten crystallization water molecules and crystallization nitric acid molecules. Further weight loss occurs at 360°C, which corresponds to the decomposition temperature of CB[6].

Fig. S4j. The TGA curve of compound Eu-Yb (9)

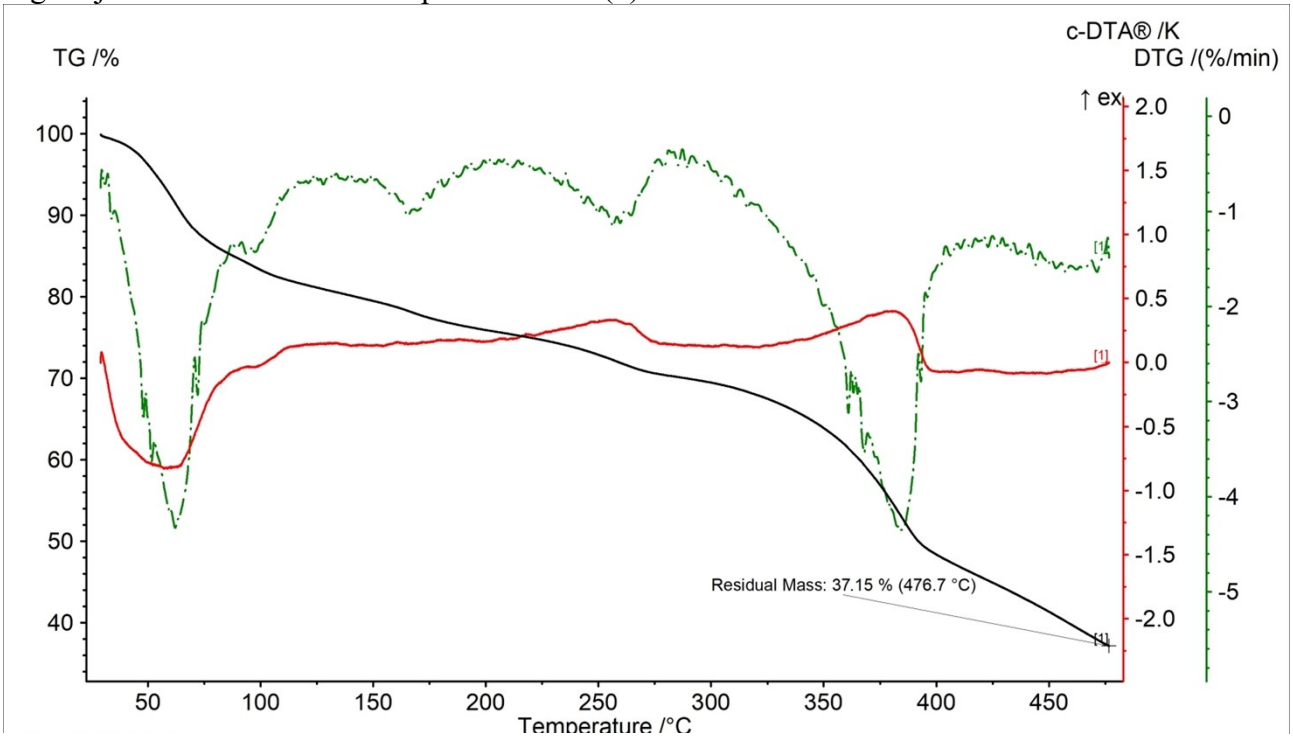

Thermal decomposition of **9** can be divided into three stages. First, desolvation occurs in the temperature range of 40–80°C and is accompanied by 15% weight loss of eleven crystallization water and nitric acid molecules. In the temperature range of 80–320°C, the sample is gradually decomposed. Further weight loss occurs at 380°C, which corresponds to the decomposition temperature of CB[6].

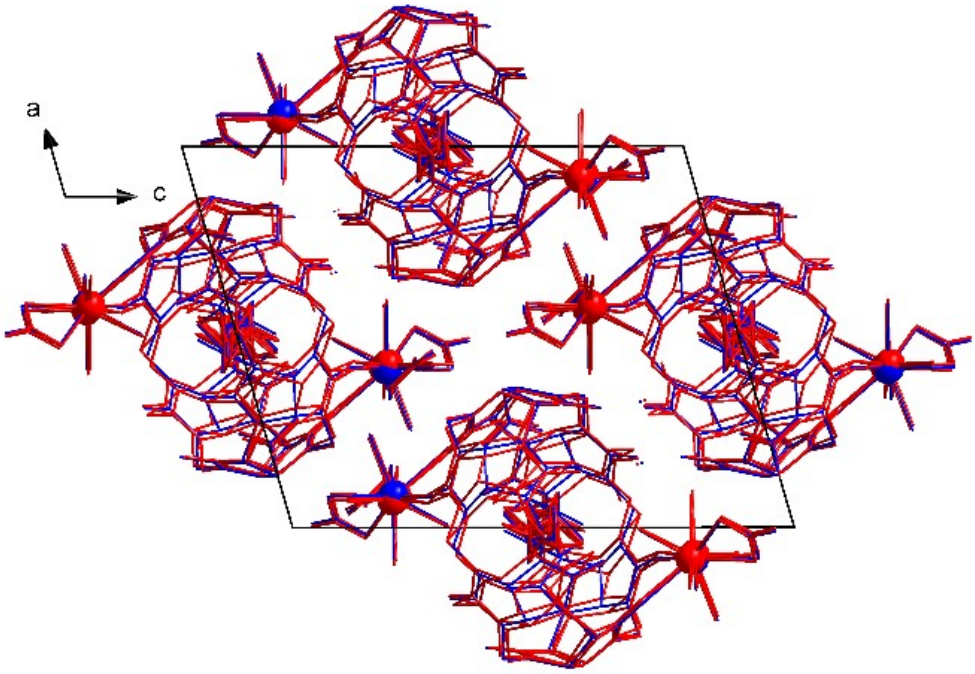

Fig. S5. An overlay of α- and β-structures showing negligible differences between them. H atoms and hydrate molecules are not shown.

Fig. S6. Schematic energy level diagram of Tb^{3+}, Eu^{3+} and Dy^{3+} ions in the complexes.

Pr (1)	Nd (2)	Sm (3)	Eu	Gd (4)	Tb (5)	Dy (6)	Ho (7)	Er (8)	Yb (9)
Mixed lanthanide samples 1:1 Eu:Ln ratio									
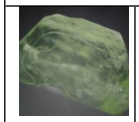						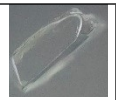			
				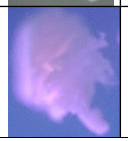				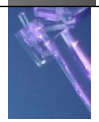	

Fig. S7. Photographs of the 365 nm ultraviolet LED lighting the crystals of compounds **1**–**9** when the LED is turned off and turned on.

Table S1. Crystal data and structure refinement for the compounds

Identification code	**1**	**2**	**3α**	**3β**	**4**	**5**	**6**	**7**	**8**	**9**
Empirical formula		$C_{36}H_{68}EuN_{31}NdO_{49}$	$C_{36}H_{68}EuN_{31}O_{49}Sm$	$C_{36}H_{68}EuN_{31}O_{49}Sm$	$C_{36}H_{68}EuGdN_{31}O_{49}$	$C_{36}H_{68}EuN_{31}O_{49}Tb$	$C_{36}H_{68}DyEuN_{31}O_{49}$	$C_{36}H_{68}Eu_{1.4}Ho_{0.6}N_{31}O_{49}$		
Formula weight		2015.41	2021.52	2021.52	2028.42	2030.09	2033.67	2030.91		
Temperature/K	150(2)	150(2)	150(2)	150(2)	150(2)	150(2)	150(2)	150(2)	150(2)	150(2)
Space group	$P2_1/n$	$P2_1/n$	$P2_1/n$	P-1	P–1	P–1	P–1	P–1	P–1	R–3
a/Å	14.3764(10)	14.4113(6)	14.4200(5)	13.4418(4)	13.4267(3)	13.4041(2)	13.4214(5)	13.4090(5)	13.429(3)	25.7946(4)
b/Å	13.6375(7)	13.6182(7)	13.5890(4)	14.4661(4)	14.4721(4)	14.4617(2)	14.4818(6)	14.4887(5)	14.477(4)	25.7946(4)
c/Å	18.0744(13)	18.0470(9)	17.9538(6)	18.2775(6)	18.2429(4)	18.2115(3)	18.2079(7)	18.2100(8)	18.244(4)	31.7638(6)
α/°	90	90	90	73.8147(10)	73.8016(10)	73.8223(13)	73.8732(13)	73.8529(14)	73.796(18)	90
β/°	105.456(3)	105.5893(16)	105.6825(13)	87.3845(11)	87.3486(10)	87.3313(13)	87.4439(13)	87.2751(14)	87.367(17)	90
γ/°	90	90	90	87.8140(9)	87.8007(11)	87.7248(12)	87.9242(12)	87.7447(12)	87.768(18)	120
Volume/Å^3	3415.5(4)	3411.5(3)	3387.14(19)	3408.45(18)	3399.26(14)	3385.45(9)	3395.3(2)	3393.2(2)	3401.3(15)	18302.9(7)
Z		2	2	2	2	2	2	2		
ρ_{calc}g/cm^3		1.962	1.982	1.970	1.982	1.991	1.989	1.988		
μ/mm^{-1}		1.803	1.916	1.904	2.021	2.095	2.147	2.117		
F(000)		2032.0	2036.0	2036.0	2040.0	2042.0	2044.0	2043.0		
Crystal size/mm^3		0.09 × 0.08 × 0.07	0.32 × 0.21 × 0.08	0.38 × 0.3 × 0.17	0.13 × 0.1 × 0.06	0.21 × 0.2 × 0.11	0.17 × 0.14 × 0.1	0.25 × 0.22 × 0.13		
Radiation		MoKα (λ = 0.71073)	MoKα (λ = 0.71073)	MoKα (λ = 0.71073)	MoKα (λ = 0.71073)	Mo Kα (λ = 0.71073)	MoKα (λ = 0.71073)	MoKα (λ = 0.71073)		
2Θ range for data collection/°		3.226 to 57.392	3.228 to 61.014	2.932 to 61.076	3.758 to 59.15	3.764 to 58.2	2.928 to 59.238	2.928 to 63.06		
Index ranges		-19 ≤ h ≤ 17, -18 ≤ k ≤ 18, -24 ≤ l ≤ 24	-20 ≤ h ≤ 20, -19 ≤ k ≤ 19, -22 ≤ l ≤ 25	-19 ≤ h ≤ 18, -20 ≤ k ≤ 20, -26 ≤ l ≤ 26	-18 ≤ h ≤ 18, -20 ≤ k ≤ 20, -25 ≤ l ≤ 25	-17 ≤ h ≤ 13, -17 ≤ k ≤ 19, -24 ≤ l ≤ 21	-18 ≤ h ≤ 18, -20 ≤ k ≤ 20, -25 ≤ l ≤ 25	-19 ≤ h ≤ 19, -20 ≤ k ≤ 21, 0 ≤ l ≤ 26		
Reflections collected		46565	65540	35598	59465	32288	32897	22195		
R_{int}, R_{sigma}		0.0311, 0.0241	0.0517, 0.0382	0.0462, 0.0713	0.0380, 0.0407	0.0228, 0.0360	0.0542, 0.0642	0.0814, 0.0800		
Data/restraints/parameters		8741/147/595	10354/117/595	35598/294/1210	18997/276/1209	15136/329/1209	32897/283/1212	22195/289/1210		
Goodness-of-fit on F^2		1.118	1.030	1.063	1.203	1.030	1.031	1.163		
Final R indexes [I>=2σ (I)]		R_1 = 0.0408, wR_2 = 0.1128	R_1 = 0.0295, wR_2 = 0.0675	R_1 = 0.0470, wR_2 = 0.1221	R_1 = 0.0453, wR_2 = 0.1010	R_1 = 0.0263, wR_2 = 0.0567	R_1 = 0.0613, wR_2 = 0.1490	R_1 = 0.0569, wR_2 = 0.1165		
Final R indexes [all data]		R_1 = 0.0455, wR_2 = 0.1173	R_1 = 0.0425, wR_2 = 0.0714	R_1 = 0.0590, wR_2 = 0.1281	R_1 = 0.0516, wR_2 = 0.1035	R_1 = 0.0335, wR_2 = 0.0603	R_1 = 0.0735, wR_2 = 0.1558	R_1 = 0.1019, wR_2 = 0.1369		
Largest diff. peak/hole / e Å^{-3}		2.78/-1.75	0.71/-0.93	2.49/-1.74	2.05/-1.55	1.16/-0.72	6.38/-2.40	1.74/-1.57		

Table S2. Ln–O bond distances in the β structures with color coding for each distance from green (large) through yellow (medium) to red (small).

Atoms		Eu-Sm (**3β**)	Eu	Eu-Gd (**4**)	Eu-Tb (**5**)	Eu-Dy (**6**)	Eu-Ho (**7**)
Ln1	O11M	2.503(3)	2.4950(18)	2.491(3)	2.485(2)	2.482(5)	2.479(5)
Ln1	O12M	2.418(3)	2.4084(18)	2.412(3)	2.3970(18)	2.401(5)	2.389(5)
Ln1	O13M	2.443(3)	2.4310(18)	2.427(3)	2.4153(18)	2.419(5)	2.405(5)
Ln1	O14M	2.445(3)	2.4337(18)	2.430(3)	2.4242(18)	2.428(5)	2.413(5)
Ln1	O15M	2.409(3)	2.3899(19)	2.390(3)	2.3774(19)	2.379(5)	2.376(5)
Ln1	O11N	2.489(3)	2.4795(17)	2.481(3)	2.467(2)	2.471(5)	2.467(5)
Ln1	O12N	2.550(3)	2.5434(18)	2.541(3)	2.533(2)	2.527(5)	2.526(5)
Ln1	O11	2.381(3)	2.3764(16)	2.377(3)	2.3665(19)	2.376(5)	2.363(4)
Ln1	O21	2.480(3)	2.4753(17)	2.474(3)	2.4700(17)	2.479(5)	2.469(4)
Ln2	O21M	2.436(3)	2.4309(18)	2.430(3)	2.414(2)	2.416(5)	2.408(5)
Ln2	O22M	2.428(3)	2.4111(18)	2.412(3)	2.4016(18)	2.404(5)	2.392(5)
Ln2	O23M	2.517(3)	2.5023(17)	2.500(3)	2.4891(19)	2.488(5)	2.479(5)
Ln2	O24M	2.407(3)	2.3946(18)	2.391(3)	2.380(2)	2.376(5)	2.368(5)
Ln2	O25M	2.429(3)	2.4188(18)	2.414(3)	2.4045(19)	2.410(5)	2.398(5)
Ln2	O21N	2.521(3)	2.5152(18)	2.516(3)	2.5067(18)	2.507(5)	2.495(5)
Ln2	O22N	2.505(3)	2.4945(17)	2.494(3)	2.4859(17)	2.483(5)	2.475(5)
Ln2	O41	2.473(3)	2.4664(17)	2.461(3)	2.4578(17)	2.462(5)	2.458(5)
Ln2	O51	2.363(3)	2.3572(17)	2.350(3)	2.3461(17)	2.342(5)	2.334(5)

Table S3. Quantum yield under different excitation.

Compound	Excitation λ_{ex}, nm				
	305	325	365	370	395
5	1	1	2	6	12
6	-	<1	-	-	1
1	-	-	<1	-	<1
2	-	-	<1	-	<1
3	-	-	<1	<1	1
4	-	<1	-	<1	2
7	-	<1	1	-	10
8	-	1	-	-	2
9	-	1	1	-	<1